MOLECULAR AND CELLULAR BIOLOGY, Sept. 2008, p. 5432–5445 Vol. 28, No. 17
0270-7306/08/$08.00+0 doi:10.1128/MCB.00307-08

Chronic Oxidative DNA Damage Due to DNA Repair Defects Causes Chromosomal Instability in *Saccharomyces cerevisiae*▽†

Natalya P. Degtyareva,[1,2] Lingling Chen,[1] Piotr Mieczkowski,[3] Thomas D. Petes,[3] and Paul W. Doetsch[1,2,4]*

Department of Biochemistry,[1] Winship Cancer Institute,[2] and Department of Radiation Oncology,[4] Emory University School of Medicine, Atlanta, Georgia 30322, and Department of Molecular Genetics and Microbiology, Duke University School of Medicine, Durham, North Carolina 27710[3]

Received 22 February 2008/Returned for modification 28 March 2008/Accepted 24 June 2008

Oxidative DNA damage is likely to be involved in the etiology of cancer and is thought to accelerate tumorigenesis via increased mutation rates. However, the majority of malignant cells acquire a specific type of genomic instability characterized by large-scale genomic rearrangements, referred to as chromosomal instability (CIN). The molecular mechanisms underlying CIN are not entirely understood. We utilized *Saccharomyces cerevisiae* as a model system to delineate the relationship between genotoxic stress and CIN. It was found that elevated levels of chronic, unrepaired oxidative DNA damage caused chromosomal aberrations at remarkably high frequencies under both selective and nonselective growth conditions. In this system, exceeding the cellular capacity to appropriately manage oxidative DNA damage resulted in a "gain-of-CIN" phenotype and led to profound karyotypic instability. These results illustrate a novel mechanism for genome destabilization that is likely to be relevant to human carcinogenesis.

Genetic instability is a common feature acquired by cancer cells, enabling the development and progression of tumors (23). Events resulting in chromosomal instability (CIN), such as amplifications and deletions of large segments of DNA, reciprocal and nonreciprocal translocations, aneuploidy, and polyploidy, constitute the large-scale genomic aberrations that characterize the majority of human cancer cells and are thought to accelerate carcinogenesis (37). The molecular mechanisms underlying CIN remain to be elucidated and are of profound importance for understanding tumorigenesis (45). Significant effort has been invested in the search for genes that when inactivated result in genome destabilization and subsequent, rapid tumor development. Such genes include those controlling the mitotic checkpoint and sister-chromatid separation (26). Most of the studies investigating the mechanisms, timing, and relevance of CIN in tumorigenesis have been focused on genetic or epigenetic aspects of CIN. Little is known about environmental factors that may cause and/or promote CIN during tumor development.

Exogenous (environmental) and endogenous (intracellular) oxidative DNA damage is considered to play an important role in cancer etiology (25). Chronic inflammation involving the release of free radicals by leukocytes, acquired through chemical insults or viral and bacterial infections, is thought to contribute to about one in four cancers worldwide (10). Strong evidence for a direct and specific role of reactive oxygen species (ROS) in the oncogenic transformation of cells has been provided recently by the finding that the activation of two major oncogenes, the Ras and Myc oncogenes, increases intracellular levels of ROS and induces DNA damage and genomic instability (30, 54). Cells have evolved several mechanisms for the prevention and repair of oxidative damage. The base excision repair (BER) pathway is responsible for the removal of a large proportion of oxidative DNA damage, although when this pathway is inactivated or its capacity is exceeded, other repair pathways, including nucleotide excision repair (NER), recombinational repair, and translesion synthesis, contribute to the handling of the remaining lesions (14). The direct prevention of oxidative DNA damage in cells is facilitated by several pathways enabling the scavenging of ROS. Recent studies have suggested an important role for the antioxidative stress protein Tsa1p in preventing large-scale chromosomal rearrangements (24, 44).

In the present study, we employed the budding yeast *Saccharomyces cerevisiae* as a model system to address whether exceeding the cellular capacity to remove or otherwise manage the presence of oxidative DNA damage results in an increase in CIN. We addressed this issue based on the findings of our previous studies that demonstrated that cells with severely compromised capacities for BER (*ntg1*Δ *ntg2*Δ *apn1*Δ triple mutants) and NER (*rad1*Δ mutants) are able to survive under genotoxic stress from endogenous cellular sources. Despite the fact that Rad1p functions in homologous recombination, it mediates the relatively minor role of removing the heterologies during strand invasion and single-strand annealing (reviewed in reference 52). In addition, the deletion of the *TSA1* gene confers a defect in ROS scavenging. A BER- and NER-defective strain (an *ntg1*Δ *ntg2*Δ *apn1*Δ *rad1*Δ quadruple mutant) provides a unique tool for delineating the mechanisms of cellular responses to such stress, because the levels of ROS and chronic oxidative DNA damage in this strain are remarkably high, approximately equivalent to a 50% lethal acute-exposure dose (3 mM) of hydrogen peroxide (16). Such DNA repair-

* Corresponding author. Mailing address: Dept. of Biochemistry, Emory University School of Medicine, 4013 Rollins Research Center, Atlanta, GA 30322. Phone: (404) 727-0409. Fax: (404) 727-3231. E-mail: medpwd@emory.edu.

† Supplemental material for this article may be found at http://mcb.asm.org/.

▽ Published ahead of print on 30 June 2008.

TABLE 1. Heterozygous diploid strains

Strain	Relevant genotype	Plasmid[a]	Reference or source[b]
1 hDNP1	JFS989 *rad1*::*kanMX*	pFA-KMX4	56
8 hDNP1	JFS989 *rad1*::*kanMX*		
hDNP4	1 hDNP1 *ntg1*::*hphMX4*	pAG32	20
hDNP5	8 hDNP1 *ntg1*::*hphMX4*	pAG32	20
hDNP11	hDNP4 *ntg2*::*URA3*	pFL34	4
hDNP12	hDNP5 *ntg2*::*URA3*	pFL34	4
hDNP13	hDNP11 *apn1*::*TRP1*	pRS304	49
hDNP14	hDNP12 *apn1*::*TRP1*	pRS304	49
hDNP15	hDNP13 *ntg2*::*BSD*	pTEF1/Bsd	Invitrogen, Carlsbad, CA
hDNP16	hDNP14 *ntg2*::*BSD*	pTEF1/Bsd	Invitrogen, Carlsbad, CA
hDNP18	hDNP15 *DSF1*::*URA3*	pFL34	4
hDNP19	hDNP16 *DSF1*::*URA3*	pFL34	4
hDNP23	hDNP19 *tsa1*::*aur1*	pAUR112	Takara Bio Inc., Shiga, Japan
hDNP24	hDNP18 *tsa1*::*aur1*	pAUR112	Takara Bio Inc., Shiga, Japan

[a] Plasmid used for PCR amplification of the fragments for the replacement of the corresponding gene.
[b] Reference for or source of the plasmid.

deficient cells, harboring high levels of oxidative DNA damage and elevated levels of ROS, display high mutation and recombination frequencies, as well as other abnormalities, including slow growth and extreme sensitivity to DNA-damaging agents (16, 47). These findings indicate that if the levels of DNA damage exceed the capacity of the major excision repair pathways (BER and NER) to maintain the integrity of the genome, damage tolerance pathway-mediated events confer a state of genetic instability. For the present study, contour-clamped homogeneous electric field (CHEF) gel analysis of entire chromosomes was utilized to karyotype large-scale chromosomal aberrations in replicative-aging populations of subcultured haploid cells with compromised DNA repair and/or ROS-scavenging capacities. We found that even under nonselective growth conditions, cells harboring chronic oxidative DNA damage exhibited profound karyotypic changes within the genome at unexpectedly high frequencies. For strains possessing high levels of chronic, oxidative DNA damage, we also detected a "gain-of-CIN" phenotype, as well as synergistic increases in the rates of CIN in various assays for the measurement of chromosomal rearrangements, including the assessment of the rates of gross chromosomal rearrangements (GCR), chromosome loss, intrachromosomal recombination, and illegitimate mating. An analysis of the chromosomal rearrangements by comparative genome hybridization (CGH) revealed a locus for a hot spot of amplifications and deletions on chromosome II and indicated that certain genomic locations are likely to be more susceptible than others to rearrangements caused by persistent oxidative DNA damage. These results provide direct evidence that chronic oxidative DNA damage can rapidly overwhelm the abilities of cells to maintain genome integrity and have important implications for genetic instability mechanisms during the development of cancer.

MATERIALS AND METHODS

Genetic analysis and media. Genetic procedures (transformation and tetrad analysis, etc.) cell growth, and selection conditions were as described elsewhere (*Saccharomyces* Genome Database [SGD]; http://www.yeastgenome.org/). Strains were grown at 30°C. Detailed procedures for the measurement of the rates of legitimate and illegitimate mating and the rates of GCR and chromosome loss in haploids and diploids are provided in the supplemental material.

Strain construction. To avoid the accumulation of mutations in the NER-defective, BER-defective, and NER- and BER-defective haploid strain backgrounds, we constructed a series of diploid strains heterozygous for mutations in NER and/or BER genes and the *TSA1* gene. These strains were constructed by a series of consecutive transformations of the diploid strain JFS989 (a gift from Dmitry Gordenin, National Institute of Environmental Health Sciences, Research Triangle Park, NC) in which the genes of interest were disrupted with the PCR fragments containing genes for antibiotic resistance or prototrophy markers flanked by the upstream and downstream sequences of the corresponding genes (Table 1). JFS989 is a diploid constructed from the strain ALE1000 by mating-type switching. Strain ALE1000 with an intrachromosomal recombination reporter carried the 5′-truncated *lys2* sequence, and the *LEU2* gene has been integrated into chromosome II as a direct repeat with the *lys2*::*HS-D* allele, with the following resulting genotype: *MAT*α [*lys2*::Alu-DIR-*LEU2-lys2*Δ*5′*] *ade5-1 leu2-3 trp1-289 ura3-52 his7-2* (27). This strain and AMY125 (*MAT*α *ade5-1 leu2-3 trp1-289 ura3-52 his7-2*) are isogenic (28). After each transformation, the integration of the marker at the correct locus was confirmed by PCR and the dissection of 20 tetrads of the resulting diploids was carried out to confirm a 2:2 segregation of the marker. The sequences of the primers used for the generation of replacement PCR fragments are available upon request. The haploid strains used in this study (with the exception of mating-type testers and wild-type strains of different origins, used as controls) were haploid spores of hDNP18, hDNP19, hDNP23, and hDNP24 (Table 2). The diploid strains DNP101, DNP102, DNP103, and DNP104 used for chromosome loss measurements and strain JFS989 were isogenic. A detailed description of the construction of these strains is provided in the chromosome loss measurement section in the supplemental material. LCH strains are the haploid derivatives of hDNP23 and hDNP24 strains and were used for replicative-aging experiments.

The strains referred to hereinafter as BER$^-$ contained disruptions of the *NTG1*, *NTG2*, and *APN1* genes; the strains referred to as NER$^-$ contained a disruption of the *RAD1* gene; BER$^-$/NER$^-$ strains contained disruptions of all four genes. The reporter for GCR measurements (9) was constructed by placing the *URA3* gene 300 bp upstream of the *DSF1* gene on chromosome V at SGD position 19328 and approximately 14 kb from the start of the *CAN1* gene, proximal to the telomeric region. Complete genotypes of all the strains are presented in Tables 1 and 2.

Analysis of chromosomal rearrangements using CHEF gel electrophoresis, array CGH, and Southern analysis. CHEF gel electrophoresis was performed to detect large-scale chromosomal rearrangements as described previously (40). A detailed characterization of chromosomal rearrangements was carried out by array CGH (31). Details of these analyses and Southern blot hybridization and references to the Gene Expression Omnibus database are provided in the supplemental material.

RESULTS

The level of genetic instability is elevated in cells harboring chronic unrepaired oxidative DNA damage. To investigate the role of oxidative DNA damage in the induction of genetic instability, we constructed a series of strains with compromised

TABLE 2. Genotypes of the strains

Strain	Relevant genotype and/or description[a]
hDNP18	*MAT***a**/*MAT*α *rad1*::*kanMX4*/*RAD1 ntg1*::*hphMX4*/*NTG1 ntg2*::*BSD*/*NTG2 apn1*::*TRP1*/*APN1 DSF1*::*URA3*/*DSF1 his7-1*/*his7-1 lys2*Δ*5′*::*LEU-lys2*Δ*3′*/*lys2*Δ*5′*::*LEU-lys2*Δ*3′ ade5-1*/*ade5-1 trp1-289*/*trp1-289 ura3-52*/*ura3-52*
hDNP19	*MAT***a**/*MAT*α *rad1*::*kanMX*/*RAD1 ntg1*::*hphMX4*/*NTG1 ntg2*::*BSD*/*NTG2 apn1*::*TRP1*/*APN1 DSF1*::*URA3*/*DSF1 his7-1*/*his7-1 lys2*Δ*5′*::*LEU-lys2*Δ*3′*/*lys2*Δ*5′*::*LEU-lys2*Δ*3′ ade5-1*/*ade5-1 trp1-289*/*trp1-289 ura3-52*/*ura3-52*
hDNP23	hDNP19 *tsa1*::*aur1*/*TSA1*
hDNP24	hDNP18 *tsa1*::*aur1*/*TSA1*
hDNP223	Subclone of hDNP23 karyotyped by CHEF gel electrophoresis
DNP101	*MAT***a**/*MAT*α *DSF1*::*URA3*/*DSF1 MET6*/*MET6*Δ *his7-1*/*his7-1 lys2*Δ*5′*::*LEU-lys2*Δ*3′*/*lys2*Δ*5′*::*LEU-lys2*Δ*3′ ade5-1*/*ade5-1 trp1-289*/*trp1-289 ura3-52*/*ura3-52*
DNP102	*MAT***a**/*MAT*α *DSF1*::*URA3*/*DSF1 MET6*/*MET6*Δ *his7-1*/*his7-1 lys2*Δ*5′*::*LEU-lys2*Δ*3′*/*lys2*Δ*5′*::*LEU-lys2*Δ*3′ ade5-1*/*ade5-1 trp1-289*/*trp1-289 ura3-52*/*ura3-52 rad1*::*kanMX4*/*rad1*::*kanMX4*
DNP103	*MAT***a**/*MAT*α *DSF1*::*URA3*/*DSF1 MET6*/*MET6*Δ *his7-1*/*his7-1 lys2*Δ*5′*::*LEU-lys2*Δ*3′*/*lys2*Δ*5′*::*LEU-lys2*Δ*3′ ade5-1*/*ade5-1 trp1-289*/*trp1-289 ura3-52*/*ura3-52 ntg1*::*hphMX4*/*ntg1*::*hphMX4 ntg2*::*BSD*/*ntg2*::*BSD apn1*::*TRP1*/*apn1*::*TRP1*
DNP104	*MAT***a**/*MAT*α *DSF1*::*URA3*/*DSF1 MET6*/*MET6*Δ *his7-1*/*his7-1 lys2*Δ*5′*::*LEU-lys2*Δ*3′*/*lys2*Δ*5′*::*LEU-lys2*Δ*3′ ade5-1*/*ade5-1 trp1-289*/*trp1-289 ura3-52*/*ura3-52 rad1*::*kanMX4*/*rad1*::*kanMX4 ntg1*::*hphMX4*/*ntg1*::*hphMX4 ntg2*::*BSD*/*ntg2*::*BSD apn1*::*TRP1*/*apn1*::*TRP1*
snd701	Wild-type spore of hDNP223
LCH 34*	BER$^-$/NER$^-$; passage 20
LCH 89*	BER$^-$ passage 20
LCH 270*	BER$^-$/NER$^-$; passage 15
LCH 274*	BER$^-$/NER$^-$; passage 15
LCH 279*	BER$^-$/NER$^-$; passage 15
LCH 294*	BER$^-$/NER$^-$; passage 15
LCH 580*	BER$^-$/NER$^-$ *tsa1*Δ; passage 5
LCH 611*	Wild type; *tsa1*Δ; passage 10
LCH 613*	BER$^-$ *tsa1*Δ; passage 10
DNP59[b]	1225 *met17*::*hphMX4*
DSC025[c]	*MAT*α *ade2-101oc his3*Δ*200 ura3*Δ*Nco lys2*Δ*Bgl leu2-R*
W303a[c]	*MAT*α *ade2-1 his3-11,15 ura3-1 leu2-3,112 trp1-1 rad5-535 can1-100*
BY4741[c]	*MAT***a** *his3*Δ*1 ura3*Δ*0 leu2*Δ*0 met15*Δ*0*
S288c[c]	*MAT*α *SUC2 gal2 mal mel flo1 flo8-1 hap1*

[a] Unless otherwise indicated, all the strains and JFS989 are isogenic (Materials and Methods) except for changes introduced by transformations or crosses. Only differences from JFS989 are shown. Strains marked with asterisks were used in replicative-aging experiments and are haploid derivatives of hDNP23 and hDNP24.

[b] Strain DNP59 was used in illegitimate mating experiments as a tester strain. This strain and strain 1225 (MATα *his4-15 leu2 thr4 ura3-52 trp1 lys*) (31) are isogenic.

[c] Strains DSC025, W303a, BY4741, and S288c were used for the CHEF gel karyotyping experiments as control wild-type strains. Strain DSC025 is the same as SJR751 (51). Strain BY4741 was obtained from Open Biosystems, Huntsville, AL. The full genotypes of these strains and of strains W303a (http://www.yeastgenome.org/) and S288c (39) are shown.

BER (BER$^-$ strains) and NER (NER$^-$ strains) and strains in which both NER and BER were simultaneously compromised (BER$^-$/NER$^-$ strains). BER in yeast is redundant and involves proteins with overlapping specificities (14). Thus, biologically relevant, elevated levels of endogenously produced oxidative DNA damage can be achieved when several BER genes are disrupted simultaneously (16). To exclude the possibility of selection for additional mutations and modifications as a consequence of multiple gene deletions in a haploid background, we consecutively eliminated the excision repair genes and the *TSA1* gene in a wild-type diploid strain containing the reporter systems for measuring genetic/genomic instability (see Materials and Methods). We also constructed a standard reporter system (9) via the insertion of the *URA3* gene next to *CAN1* on chromosome V for measurements of GCR (see Materials and Methods). To obtain haploid strains with multiple mutations, we dissected the resulting heterozygous strain. We have previously demonstrated that in BER$^-$ strains (*ntg1*Δ *ntg2*Δ *apn1*Δ triple mutants) and BER$^-$/NER$^-$ strains (*ntg1*Δ *ntg2*Δ *apn1*Δ *rad1*Δ quadruple mutants) the levels of endogenous oxidative DNA damage are highly elevated and approximately equivalent to a 50% lethal dose (3 mM) of hydrogen peroxide for wild-type cells (16). Ntg1p and Ntg2p are N-glycosylases, homologous to *Escherichia coli* endonuclease III (3). These enzymes are involved in the initial steps of BER and provide the major cellular activities for oxidized pyrimidine repair in yeast (59). Apn1p is the major apurinic-apyrimidinic endonuclease in yeast (43) and accounts for 97% of apurinic-apyrimidinic endonuclease and 3′-phosphodiesterase activities in yeast cell extracts (6). Previous studies from our group demonstrated that there are approximately 380 DNA oxidative lesion substrates per genome in BER$^-$ strains and 1,400 DNA lesion substrates per genome in BER$^-$/NER$^-$ strains grown to mid-log phase (16).

To assess the genetic instability in strains with elevated levels of oxidative DNA damage, we employed assays allowing for the selection of large-scale chromosome aberrations, as well as a forward mutation assay (utilizing the *CAN1* locus) and an assay for intrachromosomal recombination at the *LYS2* locus. For the assessment of GCR, we measured the rates of loss of the left arm of chromosome V and whole-chromosome loss (see Materials and Methods). Newly constructed BER$^-$/NER$^-$ strains exhibited the highest recombination and forward mutation rates, as previously reported by our group for

TABLE 3. Elevated levels of genetic instability in strains with different DNA excision repair capacities[a]

DNA repair background[b]	Mutation rate (10^{-7}) (95% confidence limits)	Recombination rate (10^{-5}) (95% confidence limits)	Arm loss (GCR) rate (10^{-9}) (95% confidence limits)	Chromosome loss rate (10^{-6}) (95% confidence limits)
Wild type	4.78 (2.18–5.98)	1.69 (1.19–7.32)	1.98 (0.24–7.13)	0.59 (0.33–0.97)
NER$^-$ (*rad1*)	8.45 [2] (7.37–11.1)	2.61 [2] (2.44–2.95)	8.00 [4] (3.84–14.7)	2.82 [5] (1.58–4.65)
BER$^-$ (*ntg1 ntg2 apn1*)	88.8 [19] (32.3–150)	6.80 [4] (4.83–12.5)	8.28 [4] (4.74–13.4)	17.2 [29] (0.74–33.8)
BER$^-$/NER$^-$ (*ntg1 ntg2 apn1 rad1*)	283 [59] (217–336)	107 [63] (99.7–108)	105 [53] (74.8–144)	47.9 [81] (26.2–80.4)

[a] Median rates for mutation, recombination, arm loss (GCR), and chromosome loss were determined for 10 to 20 cultures of two independent segregants of the same genotypes described in Materials and Methods. Increases (*n*-fold) in rates over those for the wild-type strain are indicated in brackets.
[b] The compromised DNA repair pathway in each strain type is shown; mutated genes are indicated in parentheses.

independently constructed strains (Table 3) (51). The levels of large-scale rearrangements (as measured by both GCR and chromosome loss assays) in BER$^-$/NER$^-$ strains were increased dramatically compared to those in wild-type strains (Table 3). We observed a 55-fold increase for arm loss and an 80-fold increase for chromosome loss in the BER$^-$/NER$^-$ strains that contained the highest levels of unrepaired oxidative DNA damage (Table 3) (16). The synergistic effect of the simultaneous removal of BER and NER on GCR rates indicated that in the absence of BER and NER (i.e., when the level of oxidative DNA damage is extremely high), the handling of such damage by remaining DNA damage management systems leads to CIN.

Whole-chromosome loss or the loss of a chromosome arm carrying essential genes in haploid cells is a lethal event. We utilized an illegitimate-mating assay, which allows for the selection of chromosomal aberrations affecting the *MAT* locus of chromosome III (31). In contrast to conventional methods for measuring large-scale chromosomal rearrangements, this approach detects whole-chromosome and chromosome arm loss, even when such events are lethal in a haploid cell, by rescuing the cell through mating. Another advantage of this method is that it detects and distinguishes between different types of events (e.g., large-scale aberrations versus small genetic changes, such as point mutations and small deletions) in one specific locus, which minimizes sequence context-dependent differences. The mating of two *MAT*α mating type strains (illegitimate mating) is possible when the mating type locus of one of the strains is mutated, epigenetically inactivated, or physically lost as a result of arm loss, translocation, or chromosome loss. To distinguish among these possibilities, we crossed the *MAT*α haploids with the *MAT*α tester strain, which has both arms of chromosome III marked with recessive mutations (*his3* and *thr4*). In the event that mating occurred as a result of a point mutation or a small deletion in the *MAT* locus, the resulting diploids would be His$^+$ Thr$^+$ prototrophs. A diploid with the His$^+$ Thr$^-$ phenotype would indicate a nonreciprocal translocation event or the loss of the right arm of chromosome III, whereas the production of His$^-$ Thr$^-$ auxotrophs would indicate the loss of the entire chromosome (see Materials and Methods). Overall, the frequencies of illegitimate mating of strains with compromised DNA repair capacities were three- and sevenfold higher than those of the wild type for BER$^-$ and BER$^-$/NER$^-$ strains, respectively (Fig. 1). The results of these experiments strongly support the notion that the rates of chromosomal aberrations were highest in the BER$^-$/NER$^-$ strains (Table 3 and Fig. 1). Interestingly, large-scale rearrangements in these strains constituted the major class of events leading to illegitimate mating (70% of all events), whereas in all other DNA repair backgrounds tested (wild type, NER$^-$, and BER$^-$), point mutations or small deletions were the predominant events. These results indicate that when the oxidative DNA damage level in the genome exceeds the capacity of DNA excision repair systems (available or compromised), the management of the damage processed by other systems results in the induction of large-scale aberrations (CIN), as opposed to only increases in frequencies of mutations resulting from small-scale sequence changes. Importantly, the disruption of both major pathways (BER and NER) involved in the repair of oxidative DNA damage had a synergistic effect on the rates of GCR (revealed by several different assays) and intrachromosomal recombination, as well as on mutation rates, confirming that the cellular capacity in such strains to handle spontaneous DNA damage properly had been exceeded.

DNA repair and ROS-scavenging pathways interact to suppress large-scale chromosome aberrations. To investigate the capability of cells to maintain genomic integrity under chronic, endogenous oxidative stress, we constructed strains in which mutations in DNA excision repair genes were combined with a deletion of the *TSA1* gene. Tsa1p is a peroxiredoxin involved in

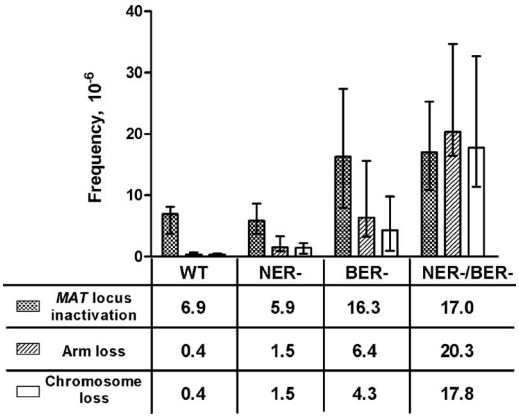

FIG. 1. Elevated levels of large-scale chromosomal aberrations in DNA excision repair-defective strains harboring elevated levels of oxidative DNA damage as measured by illegitimate-mating assays. Frequencies of each type of event were measured as described in Materials and Methods. Medians of the frequencies are indicated below the graph. Confidence limits (95%) are shown as black vertical lines. WT, wild type.

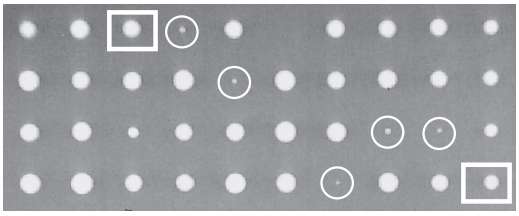

FIG. 2. DNA excision repair and ROS-scavenging pathway interactions result in severe growth defects in BER$^-$/NER$^-$ *tsa1* haploids. Shown is a representative tetrad dissection of the hDNP24 diploid strain (see Materials and Methods). Squares and circles indicate identified BER$^-$/NER$^-$ and BER$^-$/NER$^-$ *tsa1* haploids, respectively.

scavenging endogenous ROS (41, 58). Oxygen metabolism and ROS in particular are important factors leading to GCR (44). Tsa1p cooperates with several BER genes, as well as with other genes, in the suppression of GCR (24). The combined impairment of DNA excision repair and a ROS-scavenging (TSA1p-mediated) pathway preventing the introduction of oxidative DNA damage led to a severe growth defect in BER$^-$/NER$^-$ *tsa1*Δ haploids (Fig. 2), revealing strong interactions between these pathways. The *tsa1* mutants exhibited extreme sensitivity (greater than that of BER$^-$ mutants) to hydrogen peroxide but were not sensitive to hydroxyurea and methyl methanesulfonate, so it is unlikely that these mutants had significant replication defects (Fig. 3). It has also been shown recently that the anaerobic growth of *tsa1*Δ strains results in the reduction of GCR rates (44). Taken together, these data indicate that the levels of endogenous ROS and oxidative DNA damage in BER$^-$/NER$^-$ *tsa1*Δ strains were significantly elevated. Such elevations in ROS levels led to an approximately 1,000-fold increase in GCR rates and an 80-fold increase in recombination rates (Table 4) and indicated that BER, NER, and ROS-scavenging pathways interact to suppress CIN.

Chronic elevation of endogenous DNA damage levels accelerates events leading to chromosomal aberrations in replicative-aging populations of haploid yeast cells. The employment of genetic methods selecting for chromosomal aberrations provides a gauge to estimate the degree of genetic instability (CIN); however, the biological relevance of elevations in the levels of such aberrations is unclear, because these events can be disadvantageous or lethal for the cells in which they occur. In addition, methods employing selective environments have various limitations. For example, selection for GCR events in

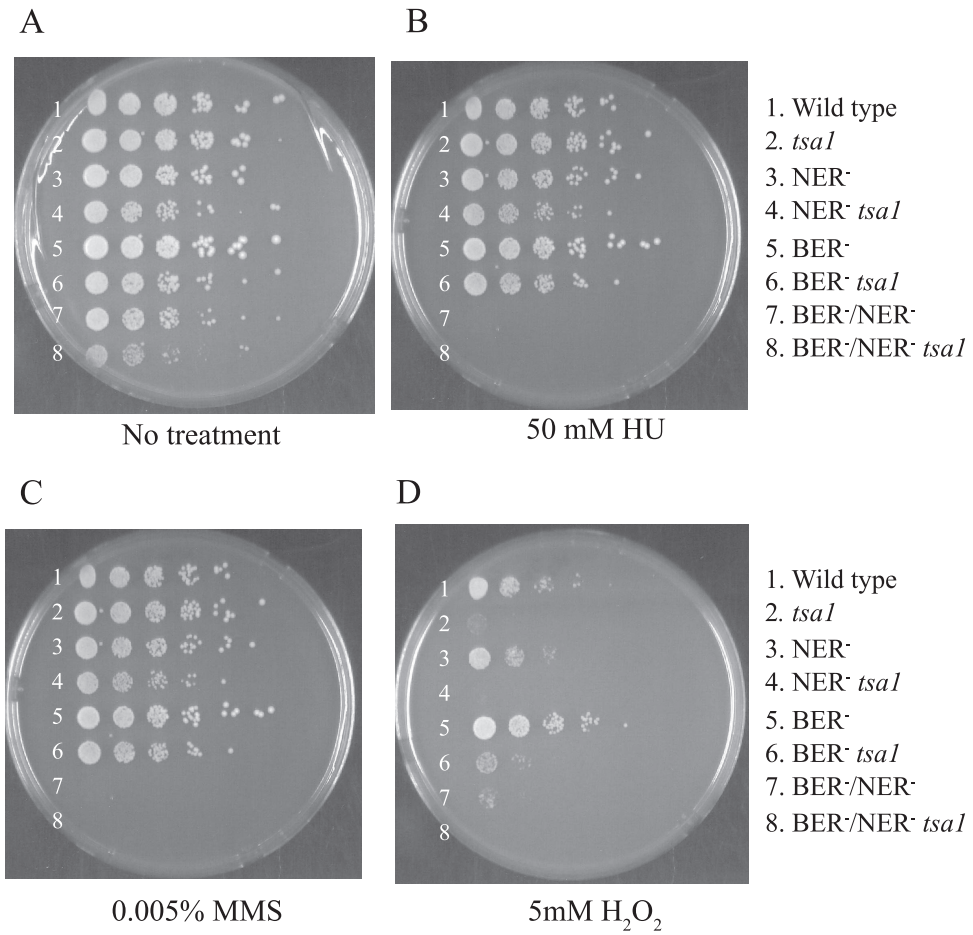

FIG. 3. Sensitivities of strains with compromised DNA excision repair and ROS scavenging to DNA-damaging agents. Equal numbers of cells were serially diluted (five times) and spotted onto rich growth medium (A) or medium containing 50 mM hydroxyurea (HU) (B), 0.005% methyl methanesulfonate (C), or 5 mM hydrogen peroxide (D). DNA repair (BER$^-$ and/or NER$^-$) and ROS-scavenging (*tsa1*Δ) backgrounds are indicated adjacent to the rows of cell dilutions.

TABLE 4. Rates of recombination and GCR in *tsa1*Δ mutants[a]

DNA repair background[b]	Recombination rate (10^{-5}) (95% confidence limits) for:		Arm loss rate (10^{-9}) (95% confidence limits) for:	
	TSA1 strains	*tsa1*Δ strains	*TSA1* strains	*tsa1*Δ strains
Wild type	0.9 (0.7–1.05)	4.7 (3.6–5.5)	0.4 (0.01–2.0)	5.8 (2.6–11)
NER$^-$ (*rad1*)	1.8 (1.4–2.7)	9.6 (8.6–11.1)	3.6 (2.0–6.0)	14.4 (9.5–20.9)
BER$^-$ (*ntg1 ntg2 apn1*)	5.2 (3.8–5.6)	21.2 (15.7–25.4)	2.8 (1.0–6.2)	8.7 (4.5–15.2)
BER$^-$/NER$^-$ (*ntg1 ntg2 apn1 rad1*)	111 (97.8–135)	72.7 (46–109)	76.7 (50.9–111)	401 (45–608)

[a] Median rates for recombination and arm loss (GCR) were determined for 10 to 20 cultures of two independent segregants of the same genotypes described in Materials and Methods.
[b] Compromised DNA excision repair pathways are shown. The genes that were mutated in order to disable each DNA repair pathway are indicated in parentheses.

haploid strains is restricted to the detection of viable variants of rearrangements and does not reveal the entire potential spectrum of possible aberrations observed in diploid cells. On the other hand, continuous genotoxic stress caused by chronic, elevated levels of endogenous ROS may not only increase CIN but also promote the selection and clonal expansion of cells capable of robust survival. This scenario in many ways mimics the clonal expansion of an abnormal, genetically unstable cell population during tumor development and progression. To address the biological consequences of chronic, elevated levels of oxidative DNA damage in yeast cells, we monitored changes in the karyotypes of haploid DNA repair-compromised strains that had been serially passaged (subcultured) on plates with complete rich medium for multiple generations. Each subculture had a single cell progenitor, and in contrast to experiments in which the consequences of single-cell replicative aging were addressed (36), we monitored the replicative aging of entire populations of haploid yeast cells. Using CHEF gel electrophoresis, we separated the chromosomes of fresh wild-type, NER$^-$, BER$^-$, BER$^-$/NER$^-$, and isogenic *tsa1*Δ segregants (see Materials and Methods). We first characterized the karyotype of each "founder" strain and established 5 to 10 subcultures originating from a single cell in the progeny of the founder. After growth to full-size colonies resulting from multiple divisions of the original single cells, a single colony at each passage for every line was randomly picked and streaked onto a fresh plate containing rich medium. Following every five passages, CHEF gel electrophoresis analysis of genomic DNA from each subculture was performed (Fig. 4A). Representative images of ethidium bromide-stained gels are shown in Fig. 4B. We compared the chromosomal migration pattern of each cell line at a specific passage number with the migration pattern of the same cell line five passages earlier and scored visible changes in chromosome size. To estimate the rates of rearrangements per cell division (Table 5), we determined that an average colony of yeast cells (all strains except for the BER$^-$/NER$^-$ *tsa1*Δ strain) contained approximately 5×10^7 cells (data not shown), resulting from about 25 divisions of the original single cell. An average colony of BER$^-$/NER$^-$ *tsa1*Δ cells contained approximately fivefold fewer cells. Taking into account that we scored karyotypic changes every fifth passage, the rate of chromosomal aberrations for BER$^-$/NER$^-$ strains after 15 passages was calculated as follows: $32/[25*15*(20 + 19 + 19)] = 1.47 \times 10^{-3}$. In this example, the number of detected changes (32) is divided by the total number of cell divisions (calculated as the number of colony-forming divisions [25] times the number of passages [15] times the number of cell lines analyzed [20 + 19 + 19]). These data indicate that karyotypic changes arise with remarkably high frequency: greater than 1 per 1,000 cells in BER$^-$/NER$^-$ strains. It should be pointed out that we underestimated the rates of rearrangements because the majority of rearrangements occurring in the largest chromosomes (such as chromosomes XII and IV) result in size differences that cannot be resolved and detected by visual inspection of the CHEF gel. In addition, a frequent observation for BER$^-$/NER$^-$ and BER$^-$/NER$^-$ *tsa1*Δ strains was that more than one visible change in chromosome sizes had occurred. For example, in one BER$^-$/NER$^-$ subculture after passaging, the sizes of two chromosomes were changed (see lane 2 for the BER$^-$/NER$^-$ strains in the bottom panel of Fig. 4B). This situation was scored as one rearrangement event because the changes in the sizes of two chromosomes may have been caused by a single event (e.g., one reciprocal translocation), although it is possible that such changes were the result of two independent events. In addition, the karyotypes of several fresh BER$^-$/NER$^-$, BER$^-$ *tsa1*Δ, and BER$^-$/NER$^-$ *tsa1*Δ segregants were different from that of the parental diploid even at passage 0 (Table 5). Such events were not scored in calculations of the rates of rearrangements, because the rearrangement may have occurred during meiosis.

Chromosome II is highly susceptible to large-scale rearrangements in strains with elevated levels of oxidative DNA damage. Insight into the mechanisms of genome destabilization caused by the presence of unrepaired DNA damage can be deduced from the analysis of recurrent patterns of chromosome rearrangements. An analysis of large-scale chromosomal rearrangements by CHEF gel karyotyping of replicative-aging cells revealed that chromosome II is highly unstable in cells with compromised DNA excision repair and/or ROS-scavenging capacities (Table 6). Changes in the size of chromosome II occurred more often than, for example, those in chromosome III even though the CHEF gel size resolution capability was greater for chromosome III than for chromosome II due to size differences. Of 86 chromosome changes observed in our experiments, 39 involved chromosome II. Surprisingly, both decreases and increases in chromosome II size were observed (Fig. 5A). Chromosome II in strain LCH 89 was smaller than that in the wild-type strain, whereas that in strain LCH 611 was larger. These observations indicate that growth in rich medium does not impose selective pressure for the loss or amplification of the particular segment of DNA conferring a cell survival advantage or disadvantage. Therefore, the elevated frequency of aberrations reflects the extreme susceptibility of one particular genomic region to CIN. These results provide evidence

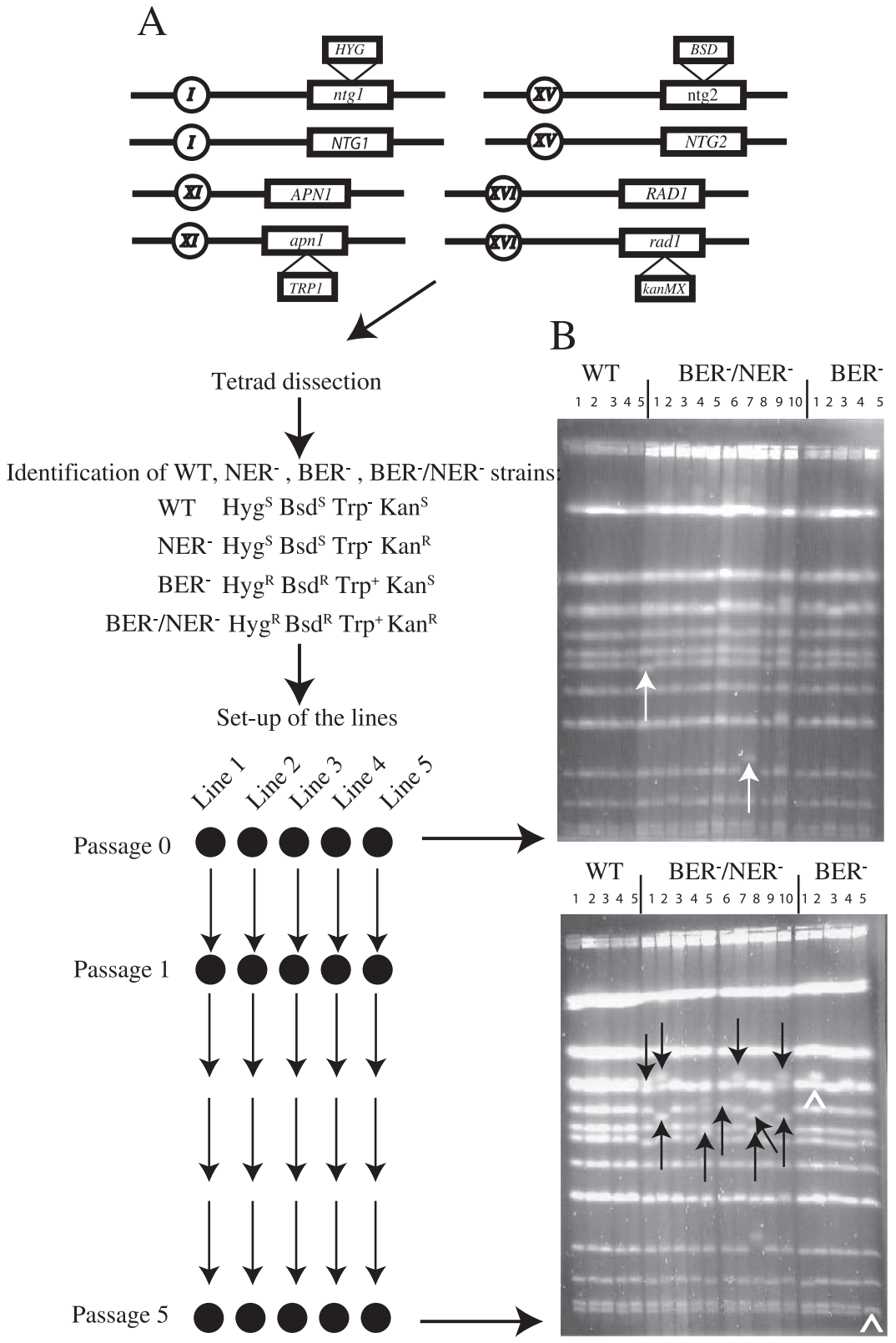

FIG. 4. Replicative aging-induced CIN in different DNA repair backgrounds (haploid cells). (A) Outline of experimental strategy (see the text for details). WT, wild type. (B) Ethidium bromide-stained CHEF gels separating yeast chromosomes at passage 0 (upper gel) and passage 5 (lower gel). White arrows indicate heterogeneity in chromosome sizes in founder cell lineages of BER$^-$/NER$^-$ strains (preexisting heterogeneity); white arrowheads indicate changes acquired by BER$^-$ lineages after five passages; black arrows indicate changes acquired by BER$^-$/NER$^-$ lineages after five passages.

TABLE 5. Frequencies of large-scale chromosomal rearrangements in haploid strains with chronic, elevated levels of endogenous oxidative DNA damage

Strain description[a]	No. of rearrangements[b] (no. of lineages analyzed) after passage:				Total no. of rearrangements (total no. of lineages analyzed)	Estimated no. of rearrangements per cell division[c] (10^{-4})
	0	5	10	15		
Wild type	0 (10)	0 (10)	1 (10)	0 (10)	1 (30)	0.9
NER$^-$	0 (10)	1 (10)	1 (10)	1 (10)	3 (30)	2.7
BER$^-$	0 (10)	3 (10)	0 (10)	3 (10)	6 (30)	5.3
BER$^-$/NER$^-$	2 (20)	8 (20)	11 (19)	13 (19)	32 (58)	14.7
tsa1	0 (10)	3 (10)	4 (10)	0 (9)	7 (29)	6.4
NER$^-$ *tsa1*	0 (10)	3 (10)	3 (10)	1 (9)	7 (29)	6.4
BER$^-$ *tsa1*	3 (10)	3 (10)	5 (8)	1 (9)	9 (27)	8.9
BER$^-$/NER$^-$ *tsa1*	8 (20)	9 (20)	6 (20)	6 (16)	21 (56)	10.0

[a] Compromised DNA excision repair pathways and *TSA1* backgrounds are shown. The genes that were mutated to disable each DNA repair pathway are the same as those listed in Table 3.
[b] Number of lineages of the indicated genotype in which changes in the sizes of different chromosomes were detected by the separation of the genomic DNA by CHEF gel electrophoresis as described in Materials and Methods.
[c] The rates of rearrangements were calculated as described in the text (see Results).

that, when cells harbor chronic, oxidative DNA damage, (i) certain chromosomal loci are more susceptible to chromosomal aberrations than others and (ii) DNA damage management at such loci can lead to different types of rearrangements, including amplifications and deletions.

Mapping rearrangements at the chromosome II CIN hot spot and analysis of the type of rearrangements by CGH. The decreased mobility of a chromosome as revealed by CHEF gel analysis can result from the amplification of a part of the chromosome, as well as from reciprocal or nonreciprocal translocation events. Similarly, increased mobility (decreased size of a chromosome) is indicative of a large deletion or translocation. To reveal the precise types of chromosome II rearrangements, we performed CGH analysis of the representative lineages from different genetic backgrounds.

We utilized CGH as a high-resolution, high-sensitivity technique for the localization and characterization of the breakpoints of chromosomal rearrangements (42). Strains with compromised DNA excision repair pathways (BER$^-$, NER$^-$, and BER$^-$/NER$^-$ strains) and/or ROS-scavenging capacities (*tsa1*Δ strains) in which changes in the size of chromosome II had been detected by CHEF gel analysis were subjected to CGH analysis. As expected, a decrease in the mobility of chromosome II corresponded to the amplification of a segment of the DNA on this chromosome and an increase in mobility corresponded to the deletion of a DNA segment (Fig. 5B). CGH analysis (see the supplemental material) also revealed that the breakpoints of rearrangements were clustered within a particular region on chromosome II (Fig. 5B and C). As indicated in the annotated SGD sequence, this DNA segment comprises a 30-kb region in close proximity to the chromosome II centromere and contains several repetitive retrotransposon sequences (*YBLCdelta7*, *YBLWsigma1*, *YBLWdelta8*, and *YBLWTy1-1*). Although it has been previously reported by several groups that these types of repetitive sequences are hot spots for chromosome rearrangements (reviewed in reference 38), only a subset of the breakpoints of deletions and amplifications identified in our study were located within such repet-

TABLE 6. Fraction of cell lineages (haploid strains) with compromised DNA excision repair and ROS-scavenging backgrounds displaying changes in the size of chromosome II

Strain description[a]	Total no. of lineages analyzed[b]	Total no. of rearrangements detected[c]	No. of lineages with chromosome II rearrangements (% of chromosome II changes)[d]	No. of lineages with chromosome III rearrangements (% of chromosome III changes)[e]
Wild type	30	1	0	0
NER$^-$	30	3	2 (67)	0
BER$^-$	30	6	1 (17)	1 (17)
BER$^-$/NER$^-$	58	32	14 (44)	4 (13)
tsa1	29	7	5 (71)	1 (14)
NER$^-$ *tsa1*	29	7	6 (86)	0
BER$^-$ *tsa1*	27	9	4 (44)	0
BER$^-$/NER$^-$ *tsa1*	56	21	7 (33)	3 (14)

[a] Compromised DNA excision repair pathways and *TSA1* backgrounds are shown. The genes that were mutated to disable each DNA repair pathway are the same as those listed in Table 3.
[b] Total number of lineages of the indicated genotype analyzed by CHEF gel electrophoresis as described in Materials and Methods.
[c] Number of lineages of the indicated genotype in which changes in the sizes of different chromosomes were detected by the separation of the genomic DNA by CHEF gel electrophoresis as described in Materials and Methods.
[d] Number of lineages of the indicated genotype in which changes in the size of chromosome II were detected by the separation of the genomic DNA by CHEF gel electrophoresis as described in Materials and Methods. The percentage of changes in the size of chromosome II relative to the changes in the sizes of all chromosomes analyzed is indicated in parentheses.
[e] Number of lineages of the indicated genotype in which changes in the size of chromosome III were detected by the separation of the genomic DNA by CHEF gel electrophoresis as described in Materials and Methods. The percentage of changes in the size of chromosome III relative to the changes in the sizes of all chromosomes analyzed is indicated in parentheses.

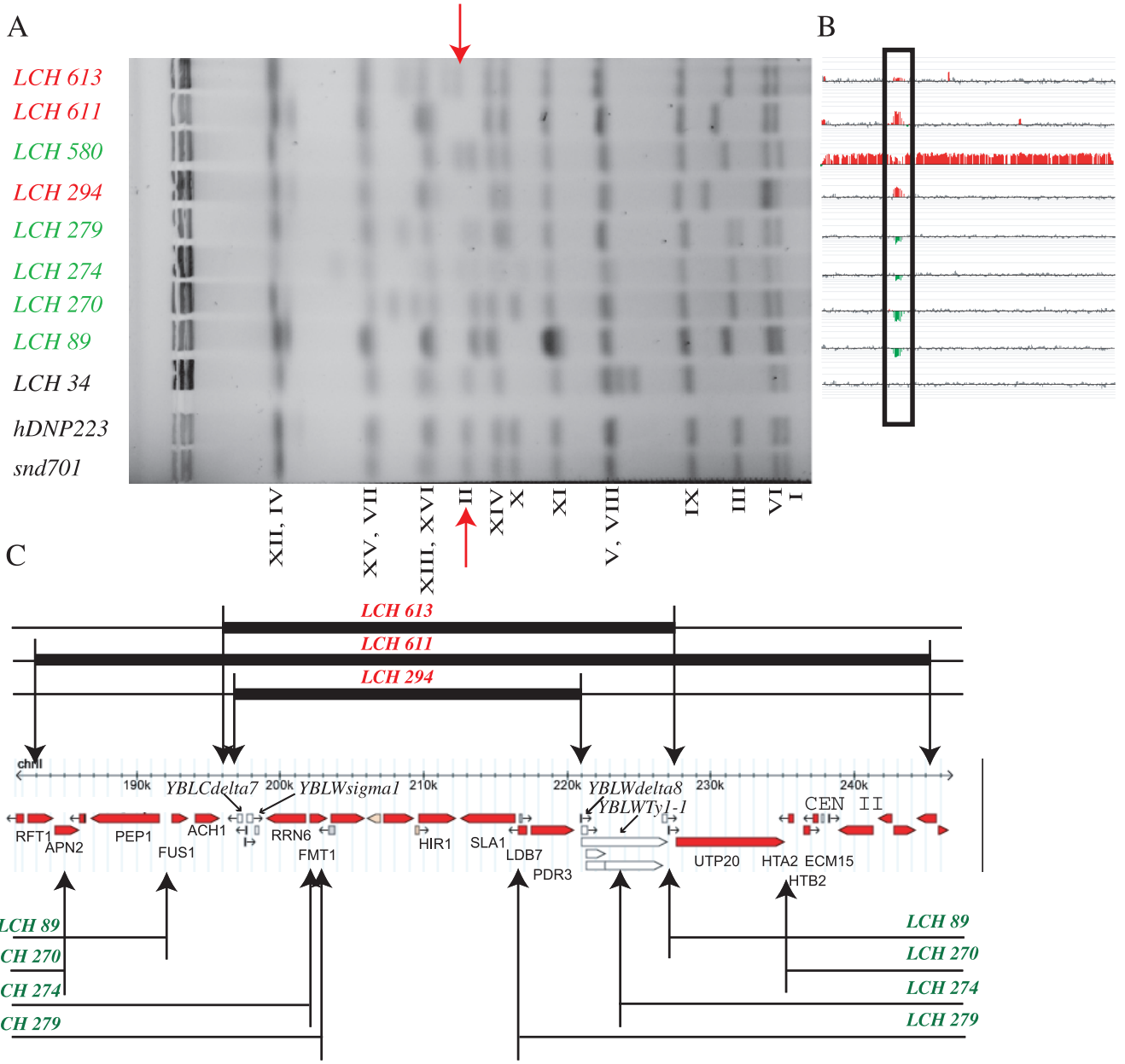

FIG. 5. Chromosome II is highly susceptible to large-scale genomic rearrangements. (A) Negative image of ethidium bromide-stained CHEF gel for representative strains with increased (green strain designations) and decreased (red strain designations) mobility of chromosome II (red arrows) compared to that of the wild type (black strain designations). Separated chromosomes are indicated by the corresponding roman numerals. Chromosomes were resolved from largest to smallest (left to right). (B) Schematic depiction of the results of CGH analysis for rearrangements of chromosome II for the corresponding (adjacent) strains (LCH 613 through LCH 34) listed in panel A. Small black vertical bars represent unchanged open reading frames (ORFs), green vertical bars indicate the deletion of ORFs, and red vertical bars indicate the amplification of ORFs. A black rectangle encloses the region of rearrangements on chromosome II. (C) Breakpoints of rearrangements within the segment of chromosome II as detected by CGH. Red horizontal pointed bars represent ORFs as annotated in the SGD (http://www.yeastgenome.org/), and white horizontal pointed bars represent repetitive sequences. The names of the ORFs are indicated in black capital letters. Black vertical arrows indicate the breakpoints of deletions (corresponding strains are listed in green) and amplifications (corresponding strains are listed in red). The genotypes of the strains are described in Table 1.

itive sequences (e.g., those in strains LCH 270 and LCH 613) (Fig. 5C). This finding suggests that the nature of DNA damage contained within a particular segment of DNA or the chromosome context of the DNA damage determines the type of rearrangement resulting in CIN. Thus, it is not unexpected that some of the resulting "signature" rearrangements on chromosome II in strains harboring chronic, oxidative DNA damage differed from those observed on chromosome III caused by decreased levels of DNA polymerases (31).

A naturally occurring duplication of chromosome II in the parental diploid strain is an informative reporter system for CIN. In our characterization of the breakpoints of rearrange-

ments, we found that in our parental heterozygous diploid hDNP223 and our wild-type haploid strain snd701, the segment of DNA between *YBLCdelta7* and *YBLWsigma1* was larger than annotated in the SGD (http://www.yeastgenome.org/) and contained a sequence highly homologous to *YBLWdelta10*, *YBLWdelta12*, *YBLWdelta8*, and *YBLWdelta9* (data not shown). In some strains with the S288c background, there is a Ty element located near *YBLCdelta7* in the Watson orientation (J. L. Argueso, personal communication), and it is likely that our strain contained this Ty element. Furthermore, chromosome II in our parental heterozygous diploid hDNP223 and wild-type strain snd701 was larger than chromosome II in several other previously described wild-type strains, e.g., S288C, W303, BY4147, and DSC025 (Fig. 6A). CGH analysis comparing the hDNP223 diploid with the W303 haploid indicated that the diploid had a duplication of an approximately 30-kb segment on the left side of chromosome II (between the Ty element near *YBLCdelta7* and *YBLWTy1-1*) and a duplication of a smaller region on the right side of the centromere (between *YBR009C* and *YBRCdelta14*). Southern blot hybridization utilizing a probe specific for the *HIR1* locus (located within the 30-kb duplication on chromosome II) confirmed that hDNP223 had two copies of this gene on each chromosome II and that S288c and W303 each had only one copy (Fig. 6B). We also found that in the isolates that had acquired a deletion on chromosome II (isolates LCH 89, LCH 270, and LCH 279), this duplication was lost (Fig. 5C). This finding was further confirmed by measurements of the density of the *HIR1* probe relative to that of a reference probe (*CSM1* locus) for chromosome III (Fig. 6B). Taken together, these results indicate that the wild-type strain employed in these studies contained a duplication of segments of chromosome II. The presence of these duplicated regions allows the detection of rearrangements that involve the deletion of essential genes and provides an informative tool for characterizing otherwise undetectable rearrangements in haploid strains. Future experiments involving the analysis of the specific DNA sequences of the breakpoints of the strains with rearrangements of chromosome II should provide a more detailed understanding of the precise nature of the molecular events leading to aberrations in cells harboring chronic, oxidative DNA damage.

DISCUSSION

"CIN" is a term used to describe a form of genetic instability (32) commonly acquired by cancer cells (23). Unlike the genetic instability caused by the inactivation of the mismatch repair system and manifested as microsatellite instability, CIN is defined as genome instability characterized by large-scale chromosome rearrangements. CIN is the predominant type of genetic instability found in human malignancies (see the Mitelman Database of Chromosome Aberrations in Cancer [http://cgap.nci.nih.gov/Chromosomes/Mitelman]), and approximately 85% of human solid tumors exhibit CIN (45). Experimental results together with mathematical modeling approaches suggest that CIN can dramatically accelerate carcinogenesis (37, 48). The molecular mechanisms underlying CIN in tumors are not entirely clear. Several proposed mechanisms leading to CIN include (i) mutation-driven defects in mitotic chromosome segregation (15, 26) and DNA double-strand break repair (57); (ii) telomere

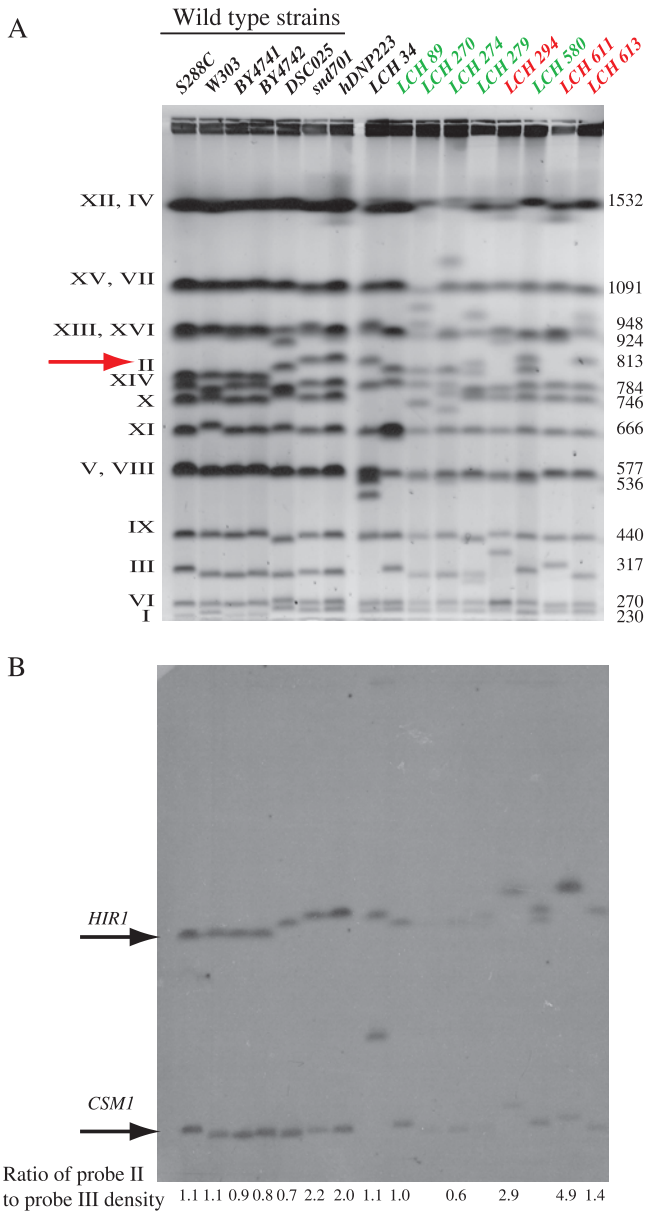

FIG. 6. Chromosome II in parental strains snd701 and hDNP223 contains an amplified DNA segment. (A) Negative image of an ethidium bromide-stained CHEF gel with resolved chromosomes from different wild-type strains and haploid progeny of hDNP223 containing rearranged forms of chromosome II. The red horizontal arrow indicates the position of chromosome II. Roman numerals to the left of the gel image indicate the positions of corresponding chromosomes. Numbers to the right of the gel image indicate the annotated size (in kilobase pairs) of the chromosomes as reported in the SGD (http://www.yeastgenome.org/). Strain designations are color coded as described in the legend to Fig. 5A. (B) Southern blot of the gel shown in panel A hybridized with probes specific to the *HIR1* (chromosome II) (Fig. 5C) and *CSM1* (chromosome III) genes. The upper horizontal arrow indicates the position of chromosome II (revealed by the *HIR1* probe), and the lower horizontal arrow indicates the position of chromosome III (revealed by the *CSM1* probe). Ratios of hybridized probe densities (probe II/probe III ratios) are indicated at the bottom of the panel.

shortening and subsequent chromosome end fusion, as well as sister-chromatid fusions, leading to recurring genome destabilization (13, 55); and (iii) the induction of rearrangements by DNA sequences containing "at-risk" motifs (ARMs) (21). ARMs include repetitive sequences that can adopt secondary structures, such as long inverted repeats (35), triplet repeats (5), and clusters of tRNA genes (1), as well as minisatellites (11). Genome destabilization by ARMs is exacerbated by events that slow down or block replication fork progression, by the corruption of checkpoint functions, and by defects in DNA double-strand break repair (1, 12). The specific types of chromosomal rearrangements are determined by the DNA sequence context of such motifs within the genome (40). The studies reported here demonstrate that exceeding the capacity of repair systems to remove oxidative DNA damage causes large-scale chromosomal rearrangements at a remarkably high frequency under nonselective growth conditions and represents a novel mechanism leading to CIN.

Elevated levels of unrepaired oxidative DNA damage are a driving force for CIN. Although it has been shown previously that the corruption of the two major DNA excision repair pathways, BER and NER, has a synergistic effect on increasing mutation and recombination rates (51), we have demonstrated for the first time that the rate of large-scale genome rearrangements (arm loss and chromosome loss) is synergistically increased in BER- and NER-defective strains (Table 3). In addition, the results from illegitimate-mating assays of these strains revealed a novel gain-of-CIN phenotype. Unlike other assays designed to detect a single, specific type of mutational event (such as chromosome loss, arm loss, recombination, or point mutations), the illegitimate-mating assay has the advantage of revealing all types of events leading to the inactivation of one specific chromosomal locus. In addition, it allows for distinguishing between small genomic changes (mutations and small deletions) and large-scale aberrations. An acquisition of the gain-of-CIN phenotype is strongly supported by the fact that combined frequencies of GCR (arm loss and chromosome loss) causing illegitimate mating were higher than the frequencies of small genetic changes leading to the inactivation of the *MAT* locus (Fig. 1). These results suggest that when the oxidative DNA damage level in the genome exceeds the capacity of the available major excision repair systems (BER and NER), DNA damage management is accommodated by other pathways that directly contribute to a large-scale mutator phenotype and genome destabilization.

The major source of oxidative DNA damage in BER- and NER-defective strains is endogenously produced ROS (16, 47). Endogenous ROS are generated as by-products of cellular metabolism or as signaling molecules (reviewed in reference 18). The extent of oxidative damage caused by endogenous and exogenous ROS is estimated to be in the order of 10,000 modifications per cell per day for the mammalian genome (34). Elevated levels of endogenous ROS are also a typical feature of malignant cells (53). An important insight into the role of ROS in the oncogenic transformation of cells is the recent finding that the activation of certain oncogenes leads to increased ROS and DNA damage (7, 54). It is important to emphasize the advantage of employing BER- and NER-defective yeast cells in our studies. Such cells exhibit substantially elevated levels of intracellular ROS (16), which facilitates addressing the role of ROS in the induction of CIN.

To further delineate the role of ROS in genome destabilization, we constructed strains in which the ability of the cells to prevent oxidative DNA damage was further compromised by the disruption of the *TSA1* gene. Tsa1p, a thioredoxin, is an antioxidative stress protein and is thought to prevent oxidative DNA damage and GCR by direct scavenging of ROS (24, 44). The impairment of both DNA excision repair pathways and Tsa1p-mediated ROS scavenging led to severe growth defects (Fig. 2), indicating interactions between the repair and scavenging pathways. At the same time, the effect of *tsa1*Δ on GCR was additive (Table 4). These findings suggest that although Tsa1p contributes to the prevention of DNA damage caused by endogenous ROS, it may also mediate other functions, such as the prevention of oxidative damage of proteins involved in genome maintenance.

Chronic, unrepaired DNA damage induces CIN, resulting in karyotypic diversity in nonselective growth environments. Large-scale chromosomal rearrangements are extremely rare events in normal (wild-type) cells, because eukaryotic as well as prokaryotic organisms have evolved multiple strategies for preventing genomic instability. The major, potentially deleterious consequences of increased CIN in dividing cell populations of multicellular organisms are not mutations or DNA rearrangements that lead to cell death but the acquisition of genetic features that enable escape from cell cycle checkpoint controls. Checkpoint surveillance systems would normally arrest cell cycle progression as soon as an excessive amount of DNA damage was sensed. Escaping such controls would confer a selective advantage for uncontrolled growth and further genetic changes. Sophisticated selective systems for the detection of certain types of rare, large-scale genomic rearrangements have been designed for model organisms, including yeast, and have been instrumental in the search for and identification of genes responsible for protecting cells from GCR (29, 50). For example, a standard system for the detection of GCR in yeast measures chromosome V arm loss and is sensitive enough to detect events occurring at frequencies of less than 10^{-9} (9). However, such selective assays for large-scale rearrangements do not reveal the biological relevance of these rare events and are limited to selection for a specific event under stringent conditions involving the context of particular chromosomes, specific DNA loci, and other features of the systems enabling the detection of the event of interest. Our results demonstrate that even under nonselective conditions, the burden of chronic, unrepaired oxidative DNA damage destabilizes the yeast genome at remarkably high frequencies, causing CIN as revealed by significant changes in chromosome sizes, and is indicative of profound karyotypic diversification. In yeast strains harboring the highest levels of oxidative damage (BER^-/NER^- and BER^-/NER^- *tsa1* strains), the absolute rates of changes in the sizes of yeast chromosomes were as high as 1 event per 1,000 cell divisions (Table 5). If similar rearrangements occur with comparable frequencies in aberrant human cell populations in an environment of elevated ROS levels (for example, in colonic epithelial cells under conditions of chronic inflammation), there is a high probability that populations of cells with diversified karyotypes will include subpopulations which have acquired growth or survival advantages. The rates of large-scale chromosomal aberrations in BER^-/NER^- and BER^-/NER^- *tsa1* strains were approximately 10-fold higher than

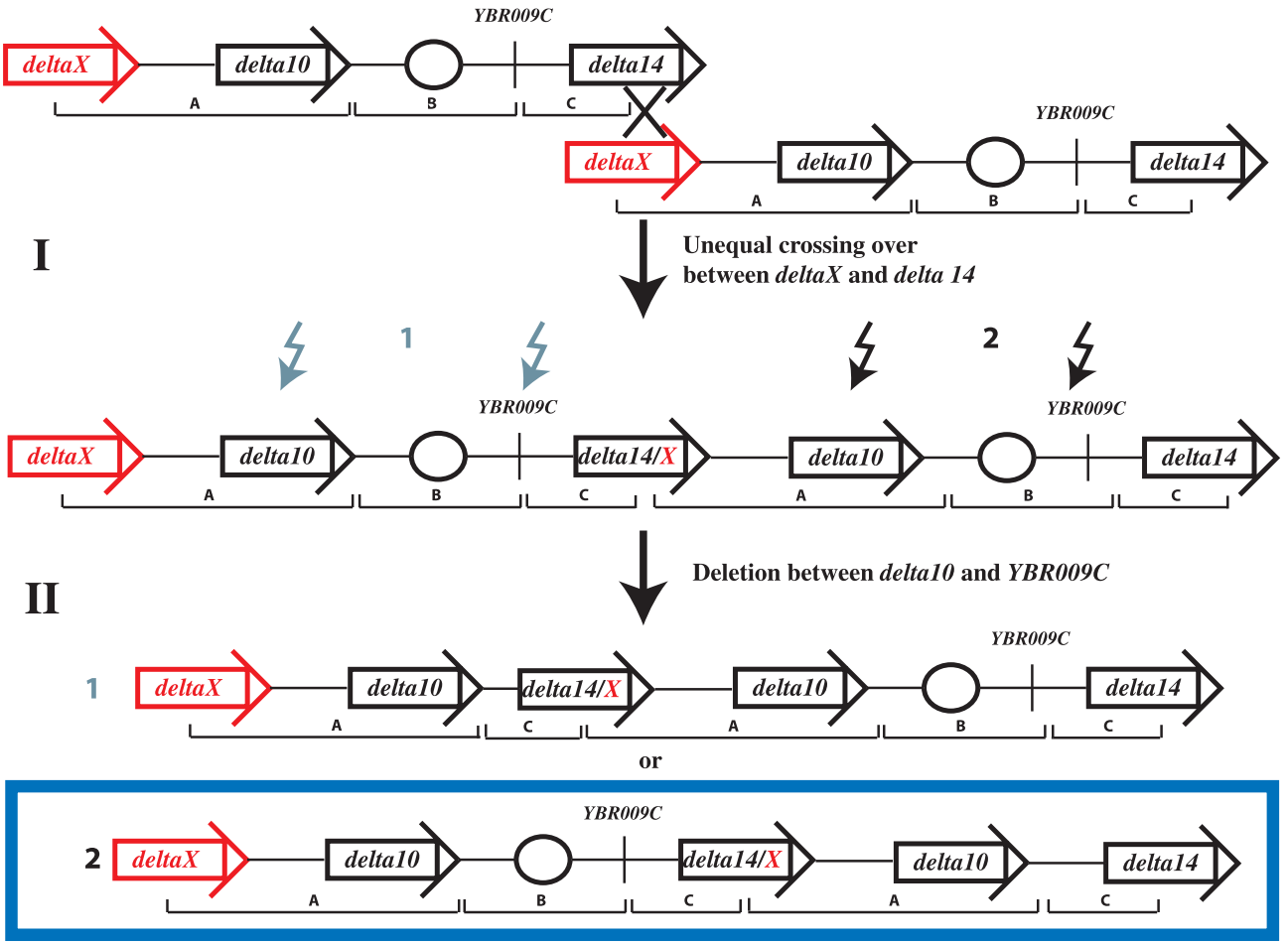

FIG. 7. Model for formation of the hot spot of large-scale rearrangements on chromosome II. Two consecutive recombination events lead to the duplication of a chromosome II segment on both sides of the centromere. (I) An unequal crossing over between an unannotated delta element (*deltaX*; red horizontal boxed arrow) located on the left arm of chromosome II and homologous *delta14*, located on the right arm of chromosome II, yields an unstable dicentric chromosome. (II) Nonhomologous end joining between *YBR009C* and *delta10* removes one of the centromeres (black circles) and stabilizes the chromosome. The deletion of the left-side centromere (gray zigzag arrows in event I diagram) produces a tandem duplication of segment A residing on one side of the centromere. Rearrangements involving such repeats would always result in the deletion or amplification of segment C, and the breakpoint of rearrangements would be located within repetitive elements. Mapping of the breakpoint of rearrangements within nonrepetitive sequences (e.g., for isolates LCH 270 and LCH 279) (Fig. 5C) provides strong support that the hot spot of rearrangements is a consequence of the deletion of the right-side centromere (black zigzag arrows in event II diagram), which results in the product shown in the blue rectangle. Repetitive elements are shown as black boxed arrows.

those in wild-type cells. The same 10-fold increase in mutation rates at the *Hprt* locus in *Msh2*-deficient mouse embryonic fibroblasts has been observed previously in studies of mutation rates in a mouse model of hereditary nonpolyposis colon cancer (46). Our findings strongly support the idea that even a moderate increase in CIN driven by oxidative DNA damage in a nonselective growth environment may trigger or promote tumorigenesis.

The CIN hot spot on chromosome II provides a novel system for revealing the molecular mechanisms leading to chromosome aberrations. ARMs have been shown to induce GCR. A common element of ARM-induced rearrangements is replication fork stalling as a result of the extrusion of DNA secondary structures and/or the involvement of specialized nucleases capable of the recognition and removal of such structures (reviewed in reference 22). We discovered a segment of chromosome II that is a hot spot for CIN in our genetic background because chromosome II had a 30-kb duplication. The changes in the size of chromosome II caused by the amplification or deletion of this segment under nonselective growth conditions were observed at remarkably elevated frequencies compared to those of changes in the sizes of the other chromosomes (Table 6). If the deletions and duplications occurred by unequal crossing over between the copies of a tandemly duplicated 30-kb segment, one would expect that all of the deletions and duplications would have the same breakpoints and that the deletion chromosome would be 30-kb smaller and the duplication chromosome would be 30-kb larger than the original chromosome II. Unlike the previously described rearrangements initiated or mediated by ARMs, the mapped boundaries of rearrangements (deletions and amplifications) within this hot spot were not exclusively associated with repetitive sequences (Fig. 5). One explanation of these findings is that the two copies of the 30-kb duplicated segment in the starting

strain resided on different sides of chromosome II (Fig. 7). Such a strain could be produced by two consecutive recombination events. First, an unequal crossover between the unannotated Ty element near *YBLCdelta7* and *YBRCdelta14* would produce a large tandem repeat and a presumably unstable dicentric chromosome. The second event would be a deletion between *YBR009C* and *YBLWdelta10* by nonhomologous end joining; such a deletion would remove the right-side centromere, stabilizing the chromosome, and result in the 30-kb duplication regions on opposite sides of the remaining centromere. We suggest that the oxidative damage-induced chromosome rearrangements may reflect an unequal crossover between these regions, resulting in a dicentric chromosome and an acentric fragment. The breakage of the dicentric chromosome, followed by deletion on one of the two centromeres, would result in the deletions and duplications observed in our study. These deletions may occur by homologous recombination involving the retrotransposon elements or by nonhomologous end joining. The latter class of event would not occur within repetitive elements. Testing this model is the goal of future experiments.

It should also be pointed out that meiotic recombination events occurring between retrotransposons on opposite sides of the centromere of chromosome II have been observed previously (33). The discovery of a duplication of a segment of chromosome II in our wild-type strains facilitated defining the events leading to oxidative DNA damage-driven CIN that would not be possible to detect using other experimental systems. If the level of unrepaired DNA damage was elevated in regions of DNA containing essential genes, high frequencies of DNA strand breaks would lead to cell death and would be undetected under selective and nonselective growth conditions. The biological relevancy of such events may be highly significant if the damage occurs in nonessential genes, which comprise one-third of the yeast genome as well as vast regions of noncoding sequences in mammalian genomes (19).

Implications for understanding the molecular mechanisms of CIN, its role in tumorigenesis, and potential therapeutic outcomes. In this study, we have demonstrated that exceeding the cellular capacity to appropriately manage chronic, oxidative DNA damage results in a new gain-of-CIN phenotype. Even though the precise role of CIN in tumorigenesis is still an issue of considerable debate, there is little doubt that the induction of large-scale genome rearrangements may facilitate the amplification of oncogenes and the deletion of tumor suppressor genes via the loss of heterozygosity, as well as the alteration of the transcriptional regulation of genes. Chronic exposure to oxidative DNA damage as a result of chronic inflammation events or exposure to exogenous ROS correlates with an increased risk of cancer (10). Our findings suggest that such increased risk may be caused by a gain-of-CIN phenotype, as revealed in this yeast model system. Although the link between defects in the repair of oxidative DNA damage and human disease states has been elusive, a recent finding implicating defects in the adenine DNA glycosylase gene *MUTYH* in human hereditary colon cancers demonstrates the important role of protection against oxidative damage in tumorigenesis (2, 8, 17). This issue is underscored by the recent finding that p53 null mice are defective in the expression of redox-regulating peroxiredoxins, resulting in increased levels of ROS (7, 30), which implies that $p53^{-/-}$ cells may be even more prone than wild-type cells to developing CIN when exposed to DNA-damaging agents.

ACKNOWLEDGMENTS

We thank Dmitry Gordenin for several yeast strains, Kirill Lobachev and Scott Devine for critical reading of the manuscript and helpful discussions, and Vidhya Narayanan and Hyun-Min Kim for assistance with CHEF gel electrophoresis.

This work was supported by NIH grants ES11163 (P.W.D.), GM24100 (T.D.P.), and GM52319 (T.D.P.).

REFERENCES

1. **Admire, A., L. Shanks, N. Danzl, M. Wang, U. Weier, W. Stevens, E. Hunt, and T. Weinert.** 2006. Cycles of chromosome instability are associated with a fragile site and are increased by defects in DNA replication and checkpoint controls in yeast. Genes Dev. **20:**159–173.
2. **Al-Tassan, N., N. H. Chmiel, J. Maynard, N. Fleming, A. L. Livingston, G. T. Williams, A. K. Hodges, D. R. Davies, S. S. David, J. R. Sampson, and J. P. Cheadle.** 2002. Inherited variants of MYH associated with somatic G:C→T:A mutations in colorectal tumors. Nat. Genet. **30:**227–232.
3. **Augeri, L., Y. M. Lee, A. B. Barton, and P. W. Doetsch.** 1997. Purification, characterization, gene cloning, and expression of Saccharomyces cerevisiae redoxyendonuclease, a homolog of Escherichia coli endonuclease III. Biochemistry **36:**721–729.
4. **Bach, M. L., F. Lacroute, and D. Botstein.** 1979. Evidence for transcriptional regulation of orotidine-5′-phosphate decarboxylase in yeast by hybridization of mRNA to the yeast structural gene cloned in Escherichia coli. Proc. Natl. Acad. Sci. USA **76:**386–390.
5. **Balakumaran, B. S., C. H. Freudenreich, and V. A. Zakian.** 2000. CGG/CCG repeats exhibit orientation-dependent instability and orientation-independent fragility in Saccharomyces cerevisiae. Hum. Mol. Genet. **9:**93–100.
6. **Boiteux, S., and M. Guillet.** 2004. Abasic sites in DNA: repair and biological consequences in Saccharomyces cerevisiae. DNA Repair (Amsterdam) **3:** 1–12.
7. **Budanov, A. V., A. A. Sablina, E. Feinstein, E. V. Koonin, and P. M. Chumakov.** 2004. Regeneration of peroxiredoxins by p53-regulated sestrins, homologs of bacterial AhpD. Science **304:**596–600.
8. **Cheadle, J. P., M. Krawczak, M. W. Thomas, A. K. Hodges, N. Al-Tassan, N. Fleming, and J. R. Sampson.** 2002. Different combinations of biallelic APC mutation confer different growth advantages in colorectal tumours. Cancer Res. **62:**363–366.
9. **Chen, C., and R. D. Kolodner.** 1999. Gross chromosomal rearrangements in Saccharomyces cerevisiae replication and recombination defective mutants. Nat. Genet. **23:**81–85.
10. **Coussens, L. M., and Z. Werb.** 2002. Inflammation and cancer. Nature **420:**860–867.
11. **Debrauwere, H., J. Buard, J. Tessier, D. Aubert, G. Vergnaud, and A. Nicolas.** 1999. Meiotic instability of human minisatellite CEB1 in yeast requires DNA double-strand breaks. Nat. Genet. **23:**367–371.
12. **Debrauwere, H., S. Loeillet, W. Lin, J. Lopes, and A. Nicolas.** 2001. Links between replication and recombination in Saccharomyces cerevisiae: a hypersensitive requirement for homologous recombination in the absence of Rad27 activity. Proc. Natl. Acad. Sci. USA **98:**8263–8269.
13. **de Lange, T.** 2005. Telomere-related genome instability in cancer. Cold Spring Harbor Symp. Quant. Biol. **70:**197–204.
14. **Doetsch, P. W., N. J. Morey, R. L. Swanson, and S. Jinks-Robertson.** 2001. Yeast base excision repair: interconnections and networks. Prog. Nucleic Acid Res. Mol. Biol. **68:**29–39.
15. **Draviam, V. M., S. Xie, and P. K. Sorger.** 2004. Chromosome segregation and genomic stability. Curr. Opin. Genet. Dev. **14:**120–125.
16. **Evert, B. A., T. B. Salmon, B. Song, L. Jingjing, W. Siede, and P. W. Doetsch.** 2004. Spontaneous DNA damage in Saccharomyces cerevisiae elicits phenotypic properties similar to cancer cells. J. Biol. Chem. **279:**22585–22594.
17. **Frosina, G.** 2004. Commentary: DNA base excision repair defects in human pathologies. Free Radic. Res. **38:**1037–1054.
18. **Fruehauf, J. P., and F. L. Meyskens, Jr.** 2007. Reactive oxygen species: a breath of life or death? Clin. Cancer Res. **13:**789–794.
19. **Goebl, M. G., and T. D. Petes.** 1986. Most of the yeast genomic sequences are not essential for cell growth and division. Cell **46:**983–992.
20. **Goldstein, A. L., and J. H. McCusker.** 1999. Three new dominant drug resistance cassettes for gene disruption in Saccharomyces cerevisiae. Yeast **15:**1541–1553.
21. **Gordenin, D. A., and M. A. Resnick.** 1998. Yeast ARMs (DNA at-risk motifs) can reveal sources of genome instability. Mutat. Res. **400:**45–58.
22. **Haber, J. E., and M. Debatisse.** 2006. Gene amplification: yeast takes a turn. Cell **125:**1237–1240.
23. **Hanahan, D., and R. A. Weinberg.** 2000. The hallmarks of cancer. Cell **100:**57–70.

24. **Huang, M. E., and R. D. Kolodner.** 2005. A biological network in Saccharomyces cerevisiae prevents the deleterious effects of endogenous oxidative DNA damage. Mol. Cell **17:**709–720.
25. **Hussain, S. P., L. J. Hofseth, and C. C. Harris.** 2003. Radical causes of cancer. Nat. Rev. Cancer **3:**276–285.
26. **Jallepalli, P. V., and C. Lengauer.** 2001. Chromosome segregation and cancer: cutting through the mystery. Nat. Rev. Cancer **1:**109–117.
27. **Jin, Y. H., R. Obert, P. M. Burgers, T. A. Kunkel, M. A. Resnick, and D. A. Gordenin.** 2001. The 3′→5′ exonuclease of DNA polymerase delta can substitute for the 5′ flap endonuclease Rad27/Fen1 in processing Okazaki fragments and preventing genome instability. Proc. Natl. Acad. Sci. USA **98:**5122–5127.
28. **Kokoska, R. J., L. Stefanovic, J. DeMai, and T. D. Petes.** 2000. Increased rates of genomic deletions generated by mutations in the yeast gene encoding DNA polymerase delta or by decreases in the cellular levels of DNA polymerase delta. Mol. Cell. Biol. **20:**7490–7504.
29. **Kolodner, R. D., C. D. Putnam, and K. Myung.** 2002. Maintenance of genome stability in Saccharomyces cerevisiae. Science **297:**552–557.
30. **Kopnin, P. B., L. S. Agapova, B. P. Kopnin, and P. M. Chumakov.** 2007. Repression of sestrin family genes contributes to oncogenic Ras-induced reactive oxygen species up-regulation and genetic instability. Cancer Res. **67:**4671–4678.
31. **Lemoine, F. J., N. P. Degtyareva, K. Lobachev, and T. D. Petes.** 2005. Chromosomal translocations in yeast induced by low levels of DNA polymerase: a model for chromosome fragile sites. Cell **120:**587–598.
32. **Lengauer, C., K. W. Kinzler, and B. Vogelstein.** 1998. Genetic instabilities in human cancers. Nature **396:**643–649.
33. **Libuda, D. E., and F. Winston.** 2006. Amplification of histone genes by circular chromosome formation in Saccharomyces cerevisiae. Nature **443:** 1003–1007.
34. **Lindahl, T.** 1993. Instability and decay of the primary structure of DNA. Nature **362:**709–715.
35. **Lobachev, K. S., A. Rattray, and V. Narayanan.** 2007. Hairpin- and cruciform-mediated chromosome breakage: causes and consequences in eukaryotic cells. Front. Biosci. **12:**4208–4220.
36. **McMurray, M. A., and D. E. Gottschling.** 2004. Aging and genetic instability in yeast. Curr. Opin. Microbiol. **7:**673–679.
37. **Michor, F., Y. Iwasa, B. Vogelstein, C. Lengauer, and M. A. Nowak.** 2005. Can chromosomal instability initiate tumorigenesis? Semin. Cancer Biol. **15:**43–49.
38. **Mieczkowski, P. A., F. J. Lemoine, and T. D. Petes.** 2006. Recombination between retrotransposons as a source of chromosome rearrangements in the yeast Saccharomyces cerevisiae. DNA Repair (Amsterdam) **5:**1010–1020.
39. **Mortimer, R. K., and J. R. Johnston.** 1986. Genealogy of principal strains of the yeast genetic stock center. Genetics **113:**35–43.
40. **Narayanan, V., P. A. Mieczkowski, H. M. Kim, T. D. Petes, and K. S. Lobachev.** 2006. The pattern of gene amplification is determined by the chromosomal location of hairpin-capped breaks. Cell **125:**1283–1296.
41. **Park, S. G., M. K. Cha, W. Jeong, and I. H. Kim.** 2000. Distinct physiological functions of thiol peroxidase isoenzymes in Saccharomyces cerevisiae. J. Biol. Chem. **275:**5723–5732.
42. **Pinkel, D., and D. G. Albertson.** 2005. Comparative genomic hybridization. Annu. Rev. Genomics Hum. Genet. **6:**331–354.
43. **Popoff, S. C., A. I. Spira, A. W. Johnson, and B. Demple.** 1990. Yeast structural gene (APN1) for the major apurinic endonuclease: homology to Escherichia coli endonuclease IV. Proc. Natl. Acad. Sci. USA **87:**4193–4197.
44. **Ragu, S., G. Faye, I. Iraqui, A. Masurel-Heneman, R. D. Kolodner, and M. E. Huang.** 2007. Oxygen metabolism and reactive oxygen species cause chromosomal rearrangements and cell death. Proc. Natl. Acad. Sci. USA **104:** 9747–9752.
45. **Rajagopalan, H., M. A. Nowak, B. Vogelstein, and C. Lengauer.** 2003. The significance of unstable chromosomes in colorectal cancer. Nat. Rev. Cancer **3:**695–701.
46. **Reitmair, A. H., R. Risley, R. G. Bristow, T. Wilson, A. Ganesh, A. Jang, J. Peacock, S. Benchimol, R. P. Hill, T. W. Mak, R. Fishel, and M. Meuth.** 1997. Mutator phenotype in Msh2-deficient murine embryonic fibroblasts. Cancer Res. **57:**3765–3771.
47. **Salmon, T. B., B. A. Evert, B. Song, and P. W. Doetsch.** 2004. Biological consequences of oxidative stress-induced DNA damage in Saccharomyces cerevisiae. Nucleic Acids Res. **32:**3712–3723.
48. **Shih, I. M., W. Zhou, S. N. Goodman, C. Lengauer, K. W. Kinzler, and B. Vogelstein.** 2001. Evidence that genetic instability occurs at an early stage of colorectal tumorigenesis. Cancer Res. **61:**818–822.
49. **Sikorski, R. S., and P. Hieter.** 1989. A system of shuttle vectors and yeast host strains designed for efficient manipulation of DNA in Saccharomyces cerevisiae. Genetics **122:**19–27.
50. **Spencer, F., S. L. Gerring, C. Connelly, and P. Hieter.** 1990. Mitotic chromosome transmission fidelity mutants in Saccharomyces cerevisiae. Genetics **124:**237–249.
51. **Swanson, R. L., N. J. Morey, P. W. Doetsch, and S. Jinks-Robertson.** 1999. Overlapping specificities of base excision repair, nucleotide excision repair, recombination, and translesion synthesis pathways for DNA base damage in Saccharomyces cerevisiae. Mol. Cell. Biol. **19:**2929–2935.
52. **Symington, L. S.** 2002. Role of RAD52 epistasis group genes in homologous recombination and double-strand break repair. Microbiol. Mol. Biol. Rev. **66:**630–670.
53. **Szatrowski, T. P., and C. F. Nathan.** 1991. Production of large amounts of hydrogen peroxide by human tumor cells. Cancer Res. **51:**794–798.
54. **Vafa, O., M. Wade, S. Kern, M. Beeche, T. K. Pandita, G. M. Hampton, and G. M. Wahl.** 2002. c-Myc can induce DNA damage, increase reactive oxygen species, and mitigate p53 function: a mechanism for oncogene-induced genetic instability. Mol. Cell **9:**1031–1044.
55. **van Steensel, B., A. Smogorzewska, and T. de Lange.** 1998. TRF2 protects human telomeres from end-to-end fusions. Cell **92:**401–413.
56. **Wach, A., A. Brachat, R. Pohlmann, and P. Philippsen.** 1994. New heterologous modules for classical or PCR-based gene disruptions in Saccharomyces cerevisiae. Yeast **10:**1793–1808.
57. **Weinstock, D. M., C. A. Richardson, B. Elliott, and M. Jasin.** 2006. Modeling oncogenic translocations: distinct roles for double-strand break repair pathways in translocation formation in mammalian cells. DNA Repair (Amsterdam) **5:**1065–1074.
58. **Wong, C. M., K. L. Siu, and D. Y. Jin.** 2004. Peroxiredoxin-null yeast cells are hypersensitive to oxidative stress and are genomically unstable. J. Biol. Chem. **279:**23207–23213.
59. **You, H. J., R. L. Swanson, C. Harrington, A. H. Corbett, S. Jinks-Robertson, S. Senturker, S. S. Wallace, S. Boiteux, M. Dizdaroglu, and P. W. Doetsch.** 1999. Saccharomyces cerevisiae Ntg1p and Ntg2p: broad specificity N-glycosylases for the repair of oxidative DNA damage in the nucleus and mitochondria. Biochemistry **38:**11298–11306.